

Ambient Noise Levels in Greece as Recorded at the Hellenic Unified Seismic Network

by C. P. Evangelidis and N. S. Melis

Abstract We investigate the characteristics of ambient noise across Greece as recorded at the Hellenic Unified Seismic Network (HUSN). Power spectral densities (PSDs) and their corresponding probability density functions (PDFs) have been estimated for 110 broadband seismic stations using the continuous waveform data for a four-year period from 2007 to 2010. Using PDFs we monitor and show network performance in terms of overall station quality and the level of noise at each site. At high frequencies (> 7 Hz), the main source of noise is cultural with strong diurnal variations. Stations with constantly increased noise levels across this band indicate poor vault construction or poor site selection and provide an indication to the network operators for possible structural improvements or even station relocations. The microseismic noise levels show a clear seasonal variation at all stations. Specifically, for the double-frequency (DF; period range 4–8 s) band, the average noise level differs between stations on the mainland and those located on the islands, reaching a value as high as 10 dB. Furthermore, the DF noise peak is observed at all of the HUSN stations, and it is correlated well with local sea wave height measurements at buoys deployed in the Aegean and the Ionian seas. This indicates that the HUSN seismic network also monitors local sea–weather conditions within a range of a few hundred kilometers. The longer period single-frequency (SF) band is affected by sea–weather conditions at much longer distances in the North Atlantic. Finally, we calculate the HUSN mode noise model (HMLNM) that represents the highest probability ambient noise level in Greece. This model is a realistic noise threshold for future seismic station installations.

Online Material: Table of seismic sensor description, and tables, figures, and movie describing microseismic noise measurements.

Introduction


Waveform data received from individual seismic stations have to be constantly assessed for their quality, because this affects considerably the earthquake monitoring capabilities of the seismic network. In order to achieve this, we need to monitor the continuous station-component waveform data and estimate their noise levels for the entire frequency spectrum that the corresponding seismic sensors resolve. If this operation is applied daily for every recorded station component, then useful assumptions can be made about every station's installation and site quality, as well as the general performance of the entire seismic network. If the recorded signal is considerably high in the so-called cultural noise band, then this indicates noisy site conditions or bad sensor installation (e.g., [McNamara and Buland, 2004](#)). For a given station and time, higher noise levels than the predominant average indicate a source of noise that probably is diurnal,

seasonal, or even temporary. The last also includes local and teleseismic earthquake sources. Therefore, a detailed noise analysis of each station has to be independently performed at different frequency bands and checked for time variations. Moreover, the correlation of various external sources with the level of seismic noise at different bands and stations gives a more specific picture of the existing ambient noise field across the entire network. This can be a useful guide for network operators on future station installations, ambient noise studies, and also new applications based on what type of physical or artificial phenomena can be recorded by broadband seismometers.

In this study, we analyze the ambient noise levels of permanent seismic stations located in Greece. After a brief description of the data and method applied, we first discuss the level of noise at higher frequencies. The microseismic

noise levels are explored for seasonal variations and correlated with weather conditions and sea gravity waves at surrounding seas and more distant oceanic sources. Finally, we produce the average minimum noise model for Greece.

Noise Analysis at the Hellenic Unified Seismic Network

During 2007 a project was initiated with the aim to link the main seismic networks that monitor seismicity in Greece into one Hellenic Unified Seismic Network (HUSN). Thus, the HUSN consists of a nationwide network operated by the National Observatory of Athens Institute of Geodynamics (NOA-IG;  see Table S1, available in the electronic supplement to this paper) with network code HL, and three regional seismic networks operated by the Universities of Athens (HA), Patras (HP), and Thessaloniki (HT), respectively (Fig. 1). The unified network has seismic stations equipped with three-component broadband seismometers. A mixture of seismic sensor types exists, including Streckheisen STS-2, Guralp 3T (120 and 360 s), 3ESP (100 s), 3ESPC (60 s), 40T (30 and 60 s), Nanometrics Trillium 120P (120 s), Trillium 40 (40 s), Lennartz Le-3D (20 s), and Geotech KS2000M

(120 s) instruments. In addition, seismic stations located in Greece and neighboring countries that belong to affiliated collaborative partner networks such as GEOFON (GeoForschungsZentrums Potsdam, Germany, network code GE) and MEDNET (Mediterranean Network, Istituto Nazionale di Geofisica e Vulcanologia, Italy, network code MN), are also included in the near real-time acquisition and processing routine as it is performed at NOA-IG.

Noise analysis is performed daily for all of the HUSN stations and the affiliated collaborative partner networks that are acquired at NOA-IG using the PASSCAL Quick Look eXtra (PQLX) software (McNamara and Boaz, 2011). The NOA-IG strong-motion sensors that are collocated in seismic stations or installed at public buildings in urban areas are also monitored. For the present study we analyze only ambient noise of the HUSN broadband seismic stations. Figure 1 shows the institute that operates each station used in this study. The majority of the monitored stations have been analyzed for a four-year period, from 2007 through 2010, but there are also stations that have been installed or become available after 2007; their analyzed periods are shorter. For each station the appropriate metadata epochs have been taken into

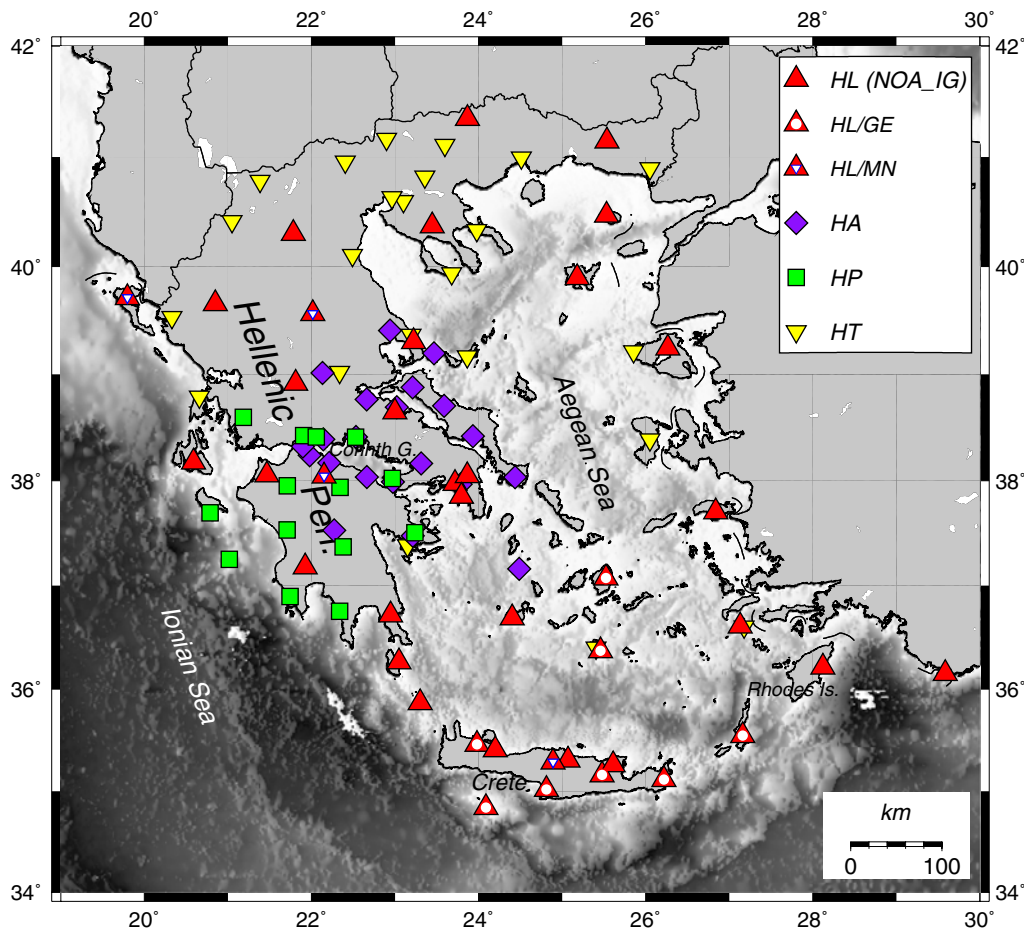


Figure 1. Map of stations used in this study. Collaborative stations are indicated with their status as they were operated until the end of 2010. The color version of this figure is available only in the electronic edition.

consideration, with any cases of uncertainty excluded from the analysis.

We use the approach described by [McNamara and Buland \(2004\)](#) by screening continuous waveform data without removing local and teleseismic earthquakes, system transients, or instrumental glitches. Using the PQLX software ([McNamara and Boaz, 2011](#)), the continuous time series of each station component is divided into 1-hr segments with 50% overlap. These segments are preprocessed by dividing them further into 13 smaller segments with 75% overlap and reducing the number of samples to the next lower power of 2. These are also transformed to a zero mean value to minimize the effect of long-period linear trends. Finally, a 10% cosine taper is applied to both ends of each segment to suppress the effect of side lobes in the fast Fourier transform (FFT). The power spectral density (PSD) of each segment is estimated via a finite-range FFT of the seismic data. The seismometer instrument response is removed from each PSD and converted into decibels with respect to acceleration for a direct comparison with the new low- or high-noise model (NLNM and NHNM) defined by [Peterson \(1993\)](#). Each 1-hr segment PSD is the average of all separate overlapping segments within it. Finally, the probability density function (PDF) of the large number of PSDs is calculated by averaging every 1/8 octave interval at discrete centered periods. For each period the average powers are stored in bins of 1 dB from -200 to -80 dB, with the PDF representing the number of powers that fall into one bin with respect to the total number in all bins. This also leads to the estimation of the minimum, tenth percentile, mean, mode, ninetieth percentile, and maximum power for each period ([McNamara and Buland, 2004](#)). Nonstationary phenomena, such as system transients, are less likely to occur, and the powers that show high probability at each period resemble the background ambient noise ([McNamara and Buland, 2004](#); [Rastin et al., 2012](#)). To ensure that data gaps due to near real-time transmission problems are not affecting the PDFs, we perform our analysis on the NOA-IG waveform database that is back-filled for possible data gaps.

High-Frequency Noise

The main source of noise across the HUSN for periods between 0.15 and 0.0625 s (~ 7 –16 Hz) is cultural ([Fig. 2](#)). This is mainly observed at stations with strong diurnal variations across this frequency band ([Fig. 2d](#)). Stations within city centers (e.g., ATH and THE), as well as remote stations such as ARG (Rhodes Island), now located within a growing village, or IGT (northwest Greece) that is located next to an active quarry, are the selected extreme examples ([Fig. 2a,b](#)). There are also stations around the Gulf of Corinth near the populated coast that show strong diurnal variations. This observation indicates a strong, noisy environment in this band, requiring possibly a station relocation. On the other hand, some stations that do not show diurnal variations across the high-frequency band ([Fig. 2d](#)) are not necessarily

quiet or well installed, because they show large, average noise levels ([Fig. 2c](#)). The IACM and SFD stations are typical examples. The first is installed in a vault that satisfies most of the general requirements of [Trnkoczy et al. \(2012\)](#), but it is located close to a water treatment facility. The second is installed on a remote island with, possibly, poor vault construction. Stations with typical seismic vault construction (e.g., IACM) ensure that the broadband seismic sensors will resolve clearly the longer period signals, even in the presence of nearby high-frequency sources. Finally, the level of noise across the high-frequency band is an indicator of possible station relocation and improvements that should be taken by the network operators.

Microseismic Noise

Microseisms are the seismic waves produced from wind-generated sea waves that through pressure fluctuations couple energy to the sea bottom. In the seismic noise spectrum two easily recognizable peaks exist at all broadband seismic stations worldwide ([Fig. 3](#)). The single-frequency peak (SF), between 10 and 16 s, matches the gravity wave periods and is generated at shallow, coastal waters either from direct pressure of ocean waves to a sloping seafloor or breaking of waves on the shoreline ([Hasselmann, 1963](#)). The double-frequency peak (DF), with higher amplitudes and shorter periods (4–8 s), is generated from nonlinear interaction of ocean gravity waves with similar wavelengths that travel in opposite directions. This generates a pressure excitation pulse at half the period of the standard water wave that propagates almost unattenuated to the ocean floor. The amplitude of the DF microseism is proportional to the product of the amplitudes of the opposing direction ocean waves ([Longuet-Higgins, 1950](#)).

We examine the microseismic noise levels across the HUSN for four consecutive years (2007–2010). For the vertical component of each station we calculate the daily mean PSD value for two different frequency bands, between 3 and 10 s for the DF band and between 10 and 16 s for the SF band ([Fig. 4](#)). Whereas the DF peak is clearly observed at all stations, the SF peak is mostly observed at stations equipped with broadband sensors with upper resolvability limits longer than 30 s and good thermal insulation ([Fig. 3](#); [E](#) see [Fig. S4](#) and [Table S1](#) in the electronic supplement).

Double-Frequency Band

The microseismic noise levels reveal, as expected, a clear sinusoidal seasonal variation for both bands, with the highest noise levels occurring during winter and the lowest levels occurring during summer ([Fig. 4](#)). Moreover, the noise levels among stations differ at these frequency bands, with more variation observed at the DF band ([Fig. 4a](#)). We compare the mean noise level during winter and summer at two representative stations located at different environments: the first established in the mainland and the second on an island

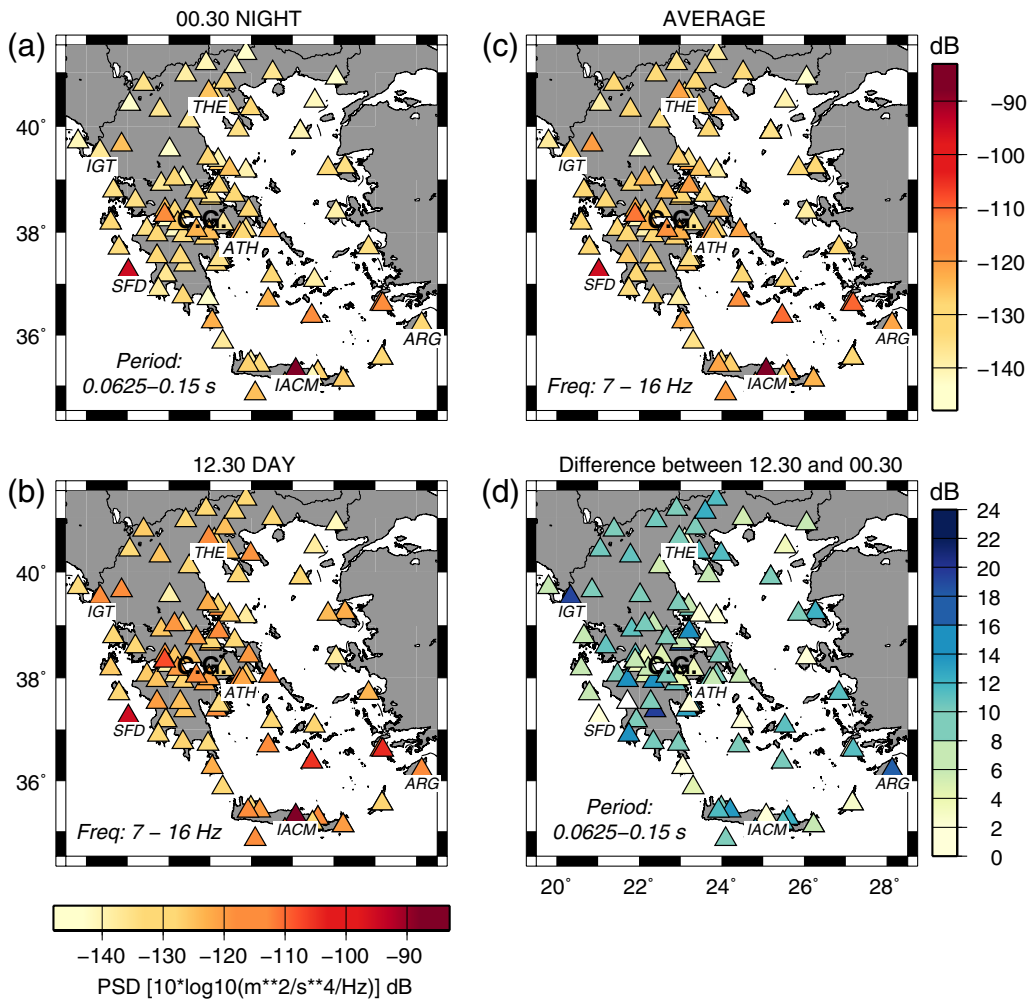


Figure 2. Maps of high-frequency noise (0.15–0.0625 s, 7–16 Hz) across the HUSN calculated: (a) at night time (00:30 GMT), (b) at day time (12:30 GMT), (c) average level, and (d) the noise difference between (a) and (b). Time periods with station malfunction are excluded. Each station is shaded according to its level of noise or noise difference in dB. Stations and areas especially mentioned in the text are also indicated; C.G., Corinth Gulf. The color version of this figure is available only in the electronic edition.

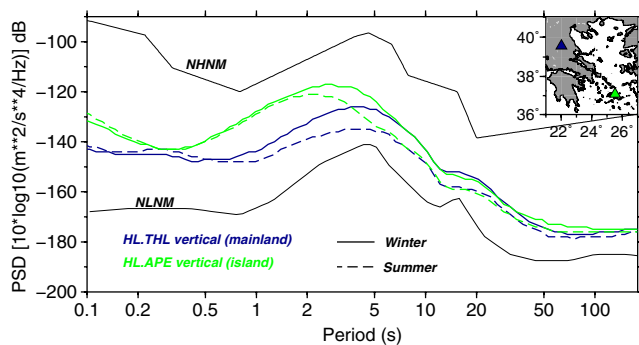


Figure 3. Mean PSD levels of the vertical component at two representative stations in mainland Greece (HL.THL) and at an island in the Aegean Sea (HL.APE). Solid lines represent mean PSDs during winter, whereas dashed lines represent mean PSDs during summer. Both stations are equipped with STS-2 sensors. Peterson (1993) new low- and high-noise models are also indicated. Inset map shows station locations in the corresponding shade. The color version of this figure is available only in the electronic edition.

in the Aegean Sea (Fig. 3). Both locations show a difference in the microseismic noise level between winter and summer reaching as much as 10 dB. The DF noise level is higher at the seismic station on the island, whereas the mainland station shows a lower level with its peak shifted to longer periods, suggesting an influence at this frequency band from the local seas. Bromirski and Duennebieer (2002) have shown that the spatial and temporal variation of DF microseism levels in near-coastal regions is directly related to wave-energy levels at nearby coastlines. Especially for the shorter periods in the DF band, between 2 and 5 s, Bromirski et al. (2005) showed a strong correlation of seismic amplitude with wind speed and direction; the produced microseismic energy attenuates within a few hundred kilometers from the source region. To verify this, we have obtained significant wave height (SWH) data from 10 buoys deployed and operated by the Hellenic Center for Marine Research (Poseidon System) for the same time period between 2007 and 2010 (stars in Fig. 5). We then estimate the average SWH value for each

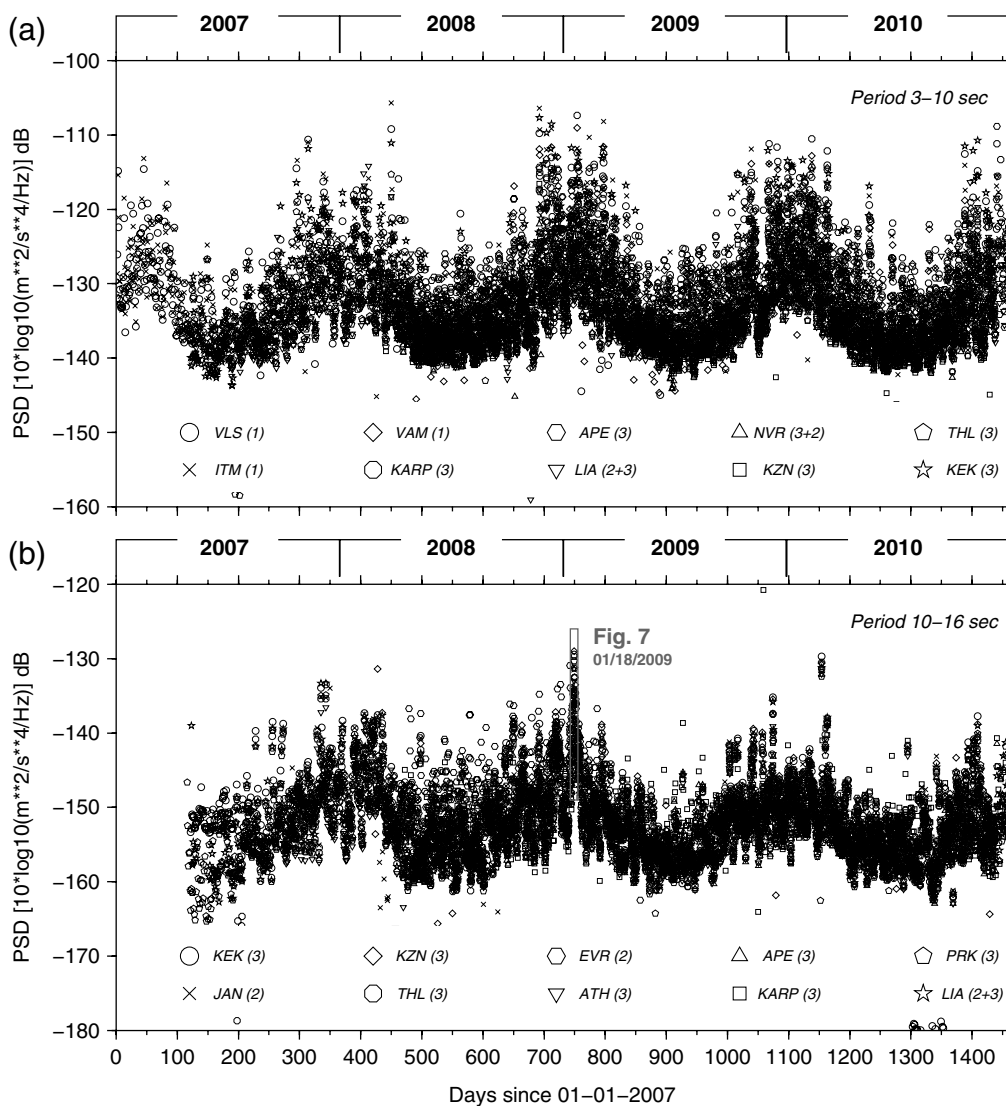


Figure 4. Seasonal variation of (a) the DF noise band (3–10 s) and (b) the SF noise band (10–16 s) for stations affiliated with the NOA-IG network (Fig. 1). Each plotted symbol represents the daily average PSD at the selected period bands for the vertical component of each station indicated in the legend. Station markings indicate the installed sensor at the period of this study with (1) Le-3D 20 s, (2) CMG-3ESPC 60 s, and (3) STS-2 120 s. Gray rectangle in (b) indicates the particular date discussed in Figure 7.

day in order to investigate similarities between SWH time series at buoys and PSD time series at broadband seismic stations within this four-year period (see Fig. S1 in the electronic supplement). We calculate the statistically significant correlation coefficient (p value $\ll 0.05$) for these two independent variables for each buoy and seismic station pair. In Figure 5, it is clearly observed that the correlation between SWH data from buoys and mean PSD values at the DF band (3–10 s) is stronger in seismic stations situated close to the buoy location. Strong correlation implies that the waves in the proximity of the buoy affect considerably the DF microseismic noise in the surrounding stations (Fig. 5a,b,e,f,h,i). For example, stations in southwestern and western Greece tend to be affected from waves in the Ionian Sea (Fig. 5h,i), and stations in Crete tend to be affected from waves in the south Aegean Sea (Fig. 5e,f). Scatter plots of correlation

coefficients versus buoy–station distance and their robust quadratic fit show that the correlation is significantly decreased with distance (Fig. 6). This decrease has the same rate for most buoys that sample a different area in the Aegean or Ionian seas. A different decreasing rate is observed for the buoy close to Mykonos Island (Fig. 6b), which is the most isolated in respect to the examined seismic station distribution (Fig. 5d). The buoy in the Gulf of Kalamata, which is not located in the open sea with high waves (Fig. 5g), does not correlate well with the observed DF noise, but also shows a decreasing pattern (Fig. 6c). In other words, SWH measurements at buoys should represent a wide open sea area in order to be correlated well with DF microseismic noise recorded at surrounding stations, within a distance of a few hundred kilometers away. Similarly, Marzorati and Bindi (2006) have concluded that the short-period DF noise in northern Italy is

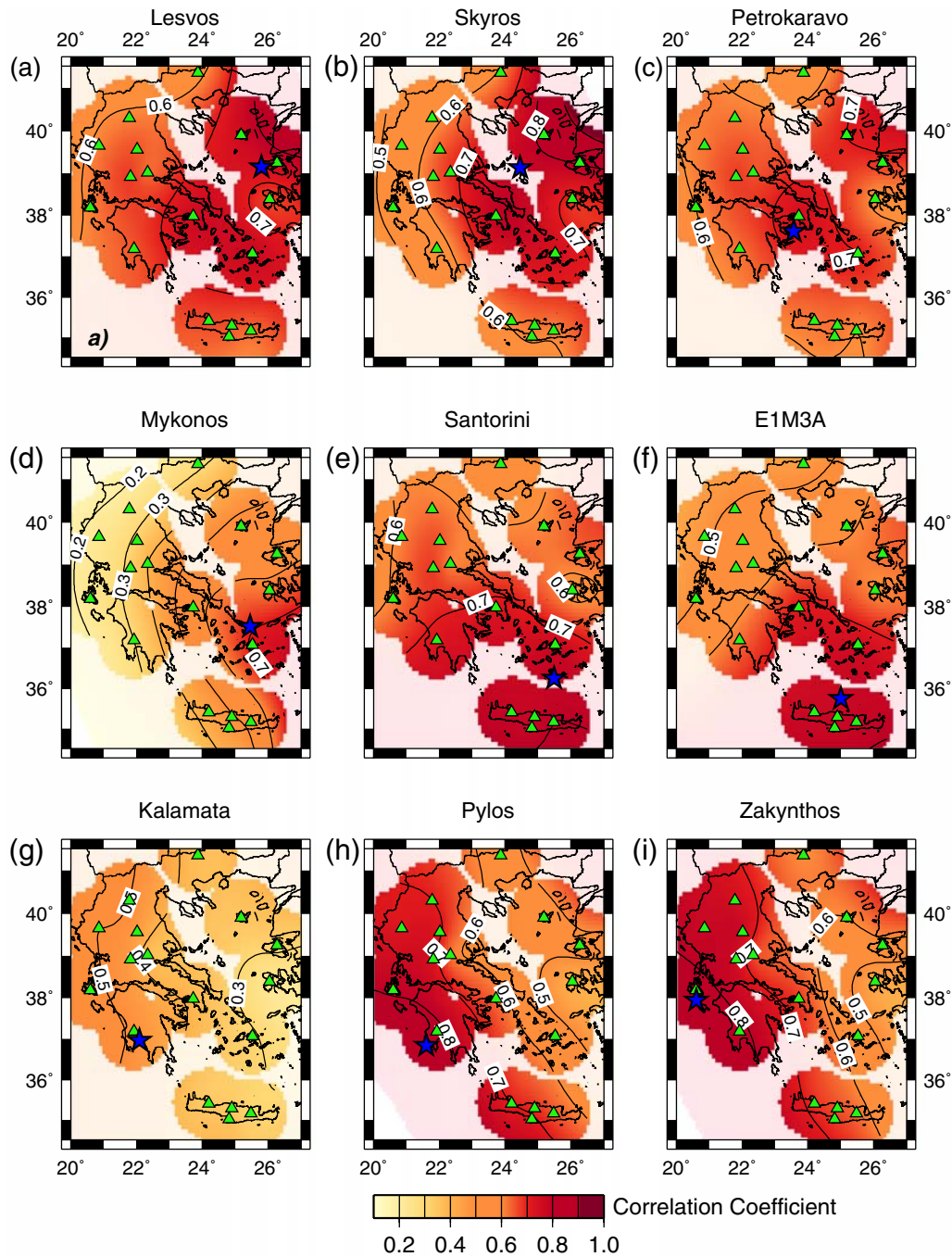


Figure 5. Maps of spatial correlation coefficient distribution between daily average SWH measurements at buoys and daily average PSD in the DF band (3–10 s) for four consecutive years (2007–2010). Each panel represents a smooth spatial correlation map between each buoy (star) and all broadband seismic stations (triangles). The correlation coefficients between all pairs of buoys and seismic stations are statistically significant because the p values are in all cases much smaller than 0.05. Panels are labeled after the buoys' names. Areas that are located farther than 100 km from the nearest seismic station are masked out to avoid unrealistic oscillations and extrapolations. The color version of this figure is available only in the electronic edition.

generated within a few hundred kilometers in the Mediterranean Sea. [Díaz *et al.* \(2010\)](#) have also shown correlation between high and low levels of DF microseismic noise in Spain with storm activity in the Atlantic waters close to Iberia, northern Morocco, and the surrounding seas. We suggest that the DF microseismic noise in Greece originates from sea

waves on the local seas, and it is well recorded at all of the HUSN stations. The existence of steep, rocky coasts in both the Aegean Sea and the Ionian Sea could be the source of this microseismic noise, as [Chevrot *et al.* \(2007\)](#) suggested elsewhere; a more detailed polarization and amplitude analysis is needed, though it is beyond the scope of this work.

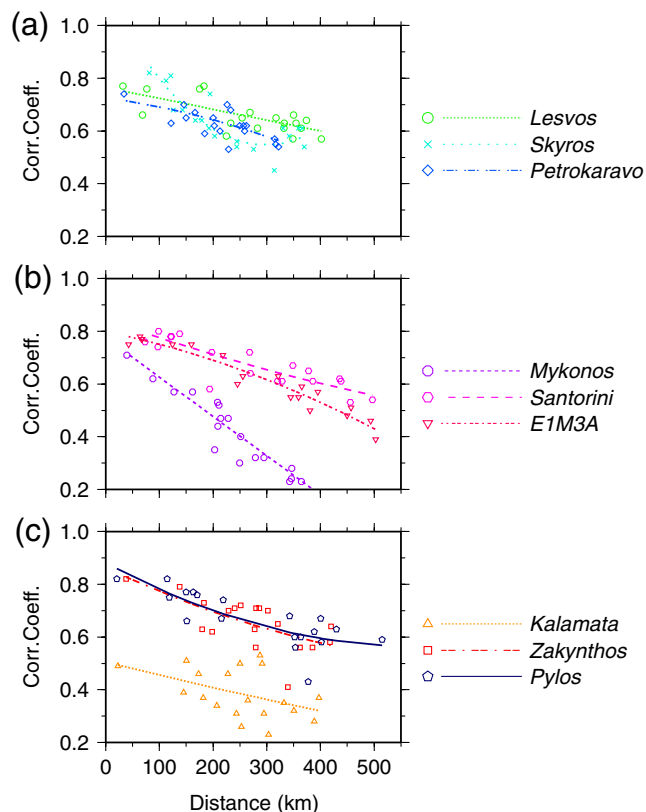


Figure 6. Scatter plots of correlation coefficients, between SWH measurements at buoys and PSD at the DF band at seismic stations for four consecutive years versus buoy–station distance. Each shape group marks a particular buoy correlated with all stations shown in Figure 5. Each different line represents a robust quadratic fit to each group. The color version of this figure is available only in the electronic edition.

Single-Frequency Band

The seasonal variation in the SF band is also clear with as much as 30 dB fluctuation between summer and winter (Fig. 4b). As Bromirski and Duennebie (2002) suggested, the highest observed SF microseism levels are generally associated with storm events and the coastal location, where the produced swells initially reach the shore, potentially at relatively long distances from the recording seismic stations. Moreover, Stehly *et al.* (2006) simultaneously analyzed data from seismic networks in California, the eastern United States, Europe, and Tanzania and identified that the main source regions of the SF microseismic noise are located in the northern Atlantic and northern Pacific during the winter, and in the Indian Ocean and southern Pacific during the summer. This suggests that the SF seismic noise is clearly related to ocean wave activity in deep water.

We explore, nonquantitatively, the origin of the SF microseism recorded across the HUSN by focusing on extremely high-noise days for this band. The highest noise levels for the examined four-year period were recorded on 18 January 2009 (Fig. 4b). On this particular date, a signifi-

cant meteorological event was under development in the northern Atlantic, as observed from the barometric maps produced by the UK Meteorological Office. Significant wave-height measurements from at least four satellite altimeter missions, validated using cross-altimeter and buoy comparison (Queffeuilou, 2004), show considerable wave heights in the North Atlantic on this day (Fig. 7a). Moreover, the SF level of noise across the HUSN stations shows a clear increasing pattern from southeast to northwest toward the North Atlantic direction (Fig. 7c). This difference in noise level from the southeast to the northwest corner is ~ 10 dB. Finally, on the same date the local weather was mild, with relatively low SWH in the Ionian and the Aegean seas (Fig. 7b). A similar trend of increasing noise from southeast to northwest is also observed during an eight-day period (15 January–23 January 2009), following the development of this significant meteorological event (see Movie S1 in the electronic supplement). The level of SF microseismic noise is reduced at the end of this period. We also examine two other dates for which significant high-noise levels are observed across this band: 22 November 2009 (see Fig. S2 in the supplement) and 9 December 2009 (see Fig. S3 in the supplement). We observe the same noise pattern and considerable wave heights in the North Atlantic. Based on all these observations, we suggest that the weather conditions in the North Atlantic and the sea gravity waves there affect clearly the observed seismic signal in the SF period band (10–16 s) at seismic broadband stations in Greece.

HUSN Mode Noise Model

Following McNamara and Buland (2004), who computed a new noise model for the continental United States, we calculate a noise model for Greece, based on the statistical mode of the PDF noise levels of all of the HUSN stations (Fig. 8; see Table S2 in the supplement). We compute, using the vertical component of each station, the noise level statistical mode from PDFs (see Fig. S5 in the supplement). The statistical mode represents the highest probability noise level at each given station. The minimum value of all station modes per octave is the new representative noise model for Greece (Fig. 8; see Table S2 in the supplement). Comparing this with the calculated mode noise model of the continental United States (UMLNM), we observe, as expected, higher noise levels at high frequencies in Greece. The absence of borehole seismometers across the HUSN increases the observed noise levels across this band due to surface anthropogenic and environmental sources. Moreover, high-frequency noise includes also the observed local seismic activity. The relatively small size of the Hellenic peninsula, in combination with the highest seismic rate observed across Europe, sets the HUSN mode noise model (HMLNM) higher than a continental model (e.g., UMLNM) for periods shorter than 2 s.

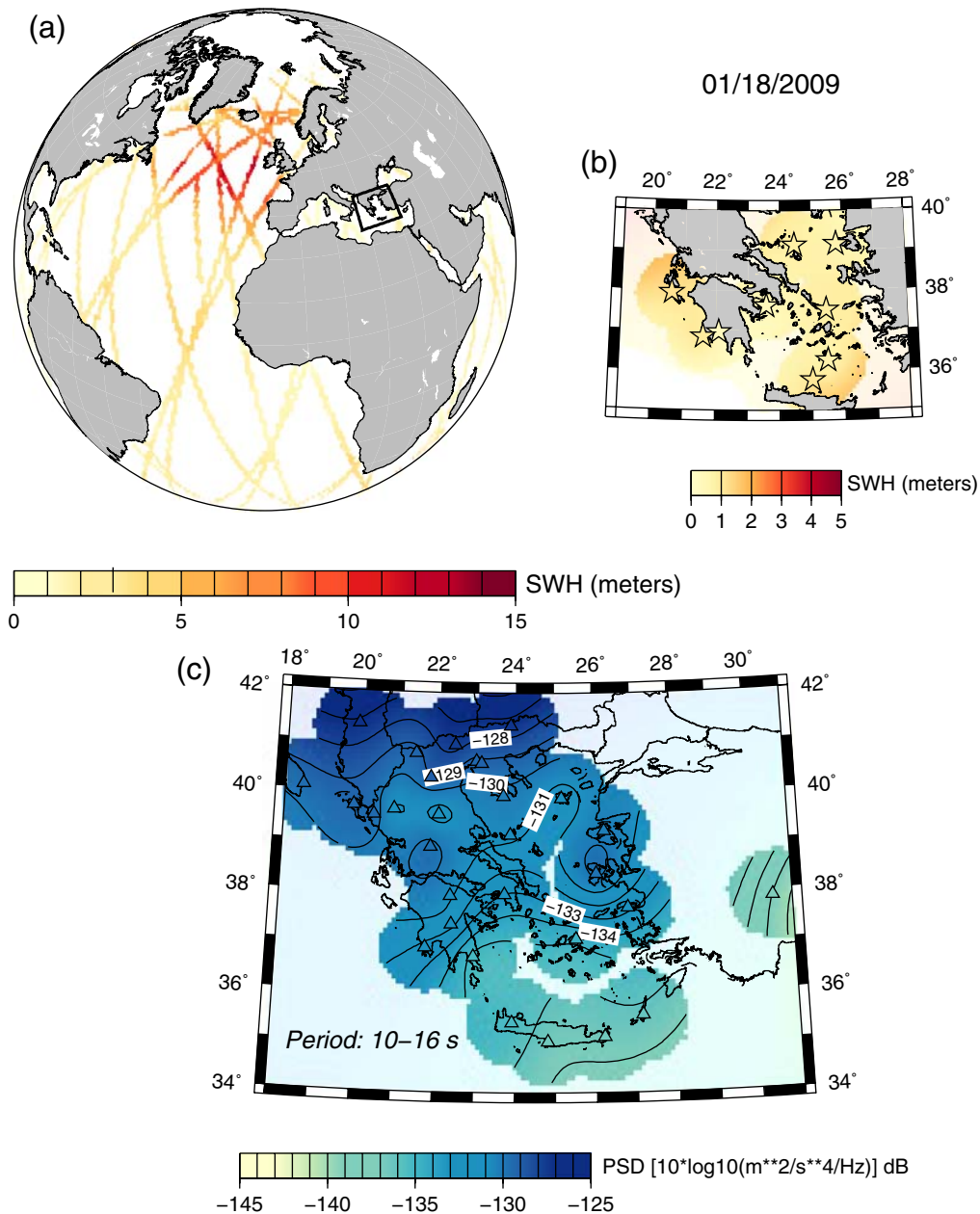


Figure 7. An example of a storm in the North Atlantic on 18 January 2009: (a) Western hemisphere validated SWH measurements from at least four satellite altimeter missions (Queffelec, 2004), (b) smooth SWH map from measurements of buoys (stars) located within the Aegean and the Ionian seas, and (c) a smooth map of the SF level of noise (10–16 s) from measurements of the HUSN seismic stations on the same date (triangles). Rectangle in (a) marks the area covered in (c). Areas in (b) and (c) that are located farther than 100 km from the nearest buoy or seismic station are masked out to avoid unrealistic oscillations and extrapolations. The color version of this figure is available only in the electronic edition.

The observed levels of microseismic noise in Greece are lower than those of the continental United States (Fig. 8). The distance between Greece and the Atlantic Ocean is greater than the distance between the central parts of the United States and both the Atlantic and Pacific oceans. However, as described in the *Double-Frequency Band* section, the microseismic noise band is strongly affected by the surrounding seas. It is evident that the microseismic noise

recorded in Greece has lower levels than the microseismic noise recorded in areas closer to oceans, especially at the SF band (Fig. 8). For periods longer than ~ 30 s, the two models are similar, indicating that this band is a global indicator, and it is not affected by local conditions.

The minimum tenth and ninetieth percentiles of the PSD distribution of all of the HUSN stations are also estimated in a similar way as the HMLNM. The gray shadowed area

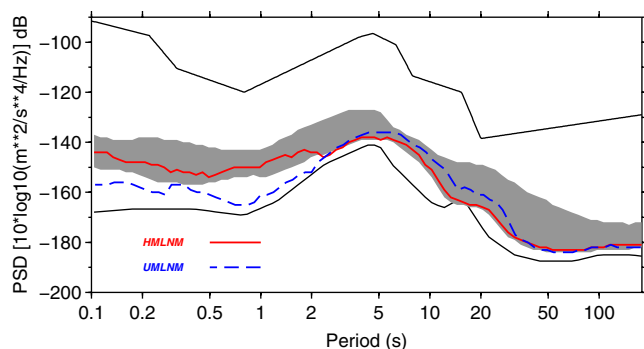


Figure 8. The HUSN PDF mode noise model (HMLNM, bold line) calculated from the minimum of all station PDF mode noise levels. The corresponding PDF mode noise model for the continental United States (UMLNM), as estimated by [McNamara and Buland \(2004\)](#), is also plotted (bold dashed line). The gray shadow marks the area between the minimum tenth and ninetieth percentiles of all of the HUSN station PSD distributions, representing the 80% confidence interval of the minimum noise levels in Greece. The color version of this figure is available only in the electronic edition.

between these two minimum levels in [Figure 8](#) represents the 80% confidence interval for the minimum noise level in Greece.

We also calculate the minimum mode, tenth percentile, and ninetieth percentile noise levels for each group of stations that have the same seismic sensor ([Fig. 9](#)). Although this is not a direct side-by-side comparison among different sensors, such as the method described by [Holcomb \(1989\)](#), it is obvious that the HMLNM model is mainly defined by the STS-2 mode noise level. [Ringler and Hutt \(2010\)](#) showed that this sensor's median and low self-noise is lower than that of other sensors. Additionally, across the HUSN, STS-2 sensors are only installed in the HL network at well-constructed and insulated vaults. The STS-2 sensors are also uniformly distributed across the country (see [Fig. S4](#) in the supplement). Station maintenance visits and site inspections have also revealed that the best insulated instruments among the same sensor group show much lower noise levels at longer periods (in [Fig. 9](#), Trillium-120P and CMG-40T groups).

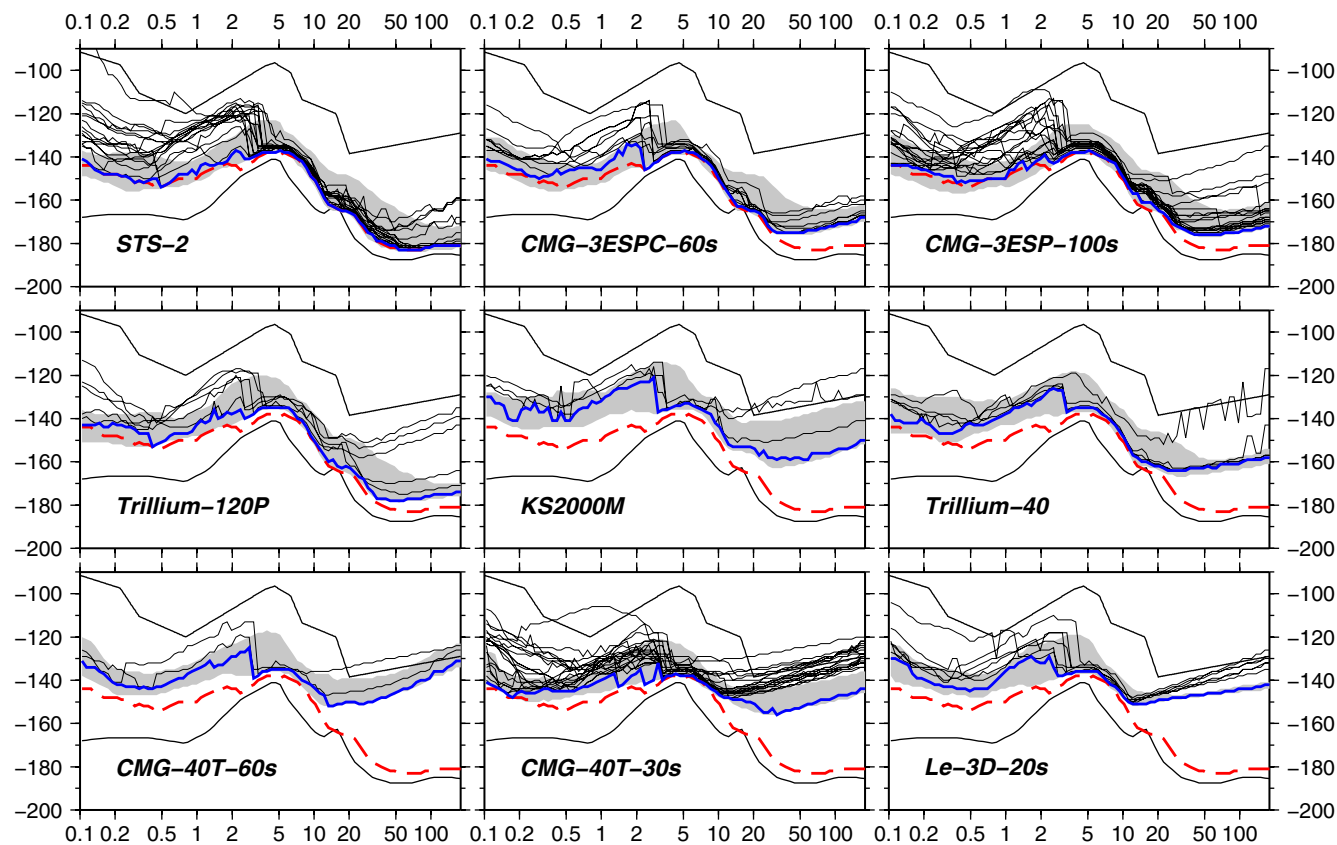


Figure 9. Minimum PDF mode noise levels for each seismic sensor group that operates in the HUSN (bold line). They are calculated as the minimum of all station individual modes (thin lines) that have the same sensor. The overall PDF mode noise model (HMLNM) of [Figure 8](#) is also plotted (bold dashed line). The gray shadow marks the area between the minimum tenth and ninetieth percentiles of the PSD distributions for each seismic sensor group, representing the 80% confidence interval of the minimum noise levels for each seismic sensor that operates in the HUSN. Units for the axes are kept the same as in [Figure 8](#) for comparison. The color version of this figure is available only in the electronic edition.

Conclusions

The main source of noise in high frequencies (~ 7 – 16 Hz) is the so-called cultural noise. This is observed as diurnal variations at stations close to populated areas. There are also seismic stations with poor vault construction and/or poor site selection that have a constant increased level of noise. Continuous monitoring across this band provides indications to the network operators of possible structural improvements or station relocations. Increased levels of noise across the high-frequency band are mostly independent of instrument type, because all the sensors operating in the HUSN have a flat instrument response across this band. This should not be confused with the usual practice of network operators to place the short-period and less expensive sensors in sites that do not satisfy most of the general requirements of Trnkoczy *et al.* (2012). When a seismic station shows increased levels of noise across this band, then site inspections and evaluations should be performed, taking into consideration the likely temporal changes of the high-frequency noise. Once a good vault and proper installation are secured, then a relatively low-cost step in order to resolve longer periods is to insulate the sensor preventing effects from abrupt thermal and atmospheric pressure fluctuations. Careful vault design, construction, and insulation ensure that the broadband seismic sensor will resolve well the longer periods, even in the presence of a nearby high-frequency noise source. This approach, assisted by the noise monitoring method used here, requires continuous adjustments and improvements by the network operators.

Microseismic noise analysis for four consecutive years (2007–2010) on the HUSN waveform data reveals a strong dependence of the DF band on the local sea conditions. The DF level of noise in Greece differs from the mainland to the islands by as much as 10 dB, but it is clearly observed and correlated at all of the HUSN stations with SWH measurements at buoys in the Aegean and the Ionian seas. Strong correlation implies that the wave heights affect considerably the observed DF microseismic noise in the surrounding stations within a range of a few hundred kilometers. Microseismic noise at longer periods (SF band) is mostly affected by sea–weather conditions at longer distances. For the analyzed time period, inspection of the highest levels of noise across this band reveals a correlation with strong North Atlantic storms with great SWHs. These results, in combination with future steps including polarization and amplitude analysis of the observed microseismic noise across the HUSN, might be useful in ambient noise tomography studies (e.g., Sabra *et al.*, 2005). Thus, interstation travel-time perturbations can be related to known geographical and seasonal variation of the microseism spectral levels (e.g., Meier *et al.*, 2010). Moreover, long-term microseismic noise observations for the longest-operating seismic stations provide an alternative metric on sea wave energy across larger and shorter time spans (e.g., Aster *et al.*, 2010, and references therein).

Finally, we calculate the HUSN mode low noise model (HMLNM) that represents the highest probability ambient noise level in Greece. Differences from the corresponding continental United States model can be attributed to the absence of borehole seismic stations in Greece that could suppress the effect of the surface high-frequency noise, the higher seismicity rate, and the reduced influence of stronger oceanic sources in the microseismic band. This model represents an optimum reference level that network operators should target for existing or future installations. The relatively increased level of noise in high frequencies indicates the need for new borehole stations that avoid the surface ground noise.

Data and Resources

Seismic waveform data used in this paper were acquired by NOAA-IG from the Hellenic Unified Seismic Network (HUSN) and the affiliated collaborative partner networks operated in Greece. Buoy data have been obtained from the Poseidon Database that offers access to the Poseidon network archived data of the Hellenic Center for Marine Research (<http://www.poseidon.hcmr.gr/>, last accessed November 2011). Satellite altimeter data were obtained from the Centre de Recherche et d'Exploitation Satellitaire, at IFREMER, Plouzan (France) (<http://cersat.ifremer.fr/Data/> and <ftp://ftp.ifremer.fr/ifremer/cersat/>, last accessed November 2011). Barometric weather maps have been obtained from the UK Meteorological Office (<http://www.metoffice.gov.uk>, last accessed January 2009). The GMT mapping software (Wessel and Smith, 1998) was used for the preparation of the figures in this paper.

Acknowledgments

We are grateful to all those scientists and scientific personnel at the National Observatory of Athens–Institute of Geodynamics, Aristotle University of Thessaloniki–Seismological Station, University of Patras–Seismological Laboratory, and National and Kapodistrian University of Athens–Seismological Laboratory for maintaining and operating their networks. This paper was supported by the NERA (Network of European Research Infrastructures for Earthquake Risk Assessment and Mitigation), an EU project financed under FP-7 Grant 262330 (CP-CSA_INFRA-2010-1.1.27). We are indebted to Associate Editor Eric P. Chael, Andrew J. Barbour, and an anonymous reviewer for their constructive comments and corrections that improved this paper.

References

- Aster, R. C., D. E. McNamara, and P. D. Bromirski (2010). Global trends in extremal microseism intensity, *Geophys. Res. Lett.* **37**, L14303, doi: [10.1029/2010GL043472](https://doi.org/10.1029/2010GL043472).
- Bromirski, P. D., and F. K. Duennebieer (2002). The near-coastal microseism spectrum: Spatial and temporal wave climate relationships, *J. Geophys. Res.* **107**, no. B8, doi: [10.1029/2001JB000265](https://doi.org/10.1029/2001JB000265).
- Bromirski, P. D., F. K. Duennebieer, and R. A. Stephen (2005). Mid-ocean microseisms, *Geochem. Geophys. Geosyst.* **6**, Q04009, doi: [10.1029/2004GC000768](https://doi.org/10.1029/2004GC000768).
- Chevrot, S., M. Sylvander, S. Benahmed, C. Ponsolles, J. M. Lefevre, and D. Paradis (2007). Source locations of secondary microseisms in

- western Europe: Evidence for both coastal and pelagic sources, *J. Geophys. Res.* **112**, B11301, doi: [10.1029/2007JB005059](https://doi.org/10.1029/2007JB005059).
- Díaz, J., A. Villaseñor, J. Morales, A. Pazos, D. Córdoba, J. Pulgar, J. L. García-Lobón, M. Harnafi, R. Carbonell, J. Gallart, and Topolberia Seismic Working Group (2010). Background noise characteristics at the IberArray broadband seismic network, *Bull. Seismol. Soc. Am.* **100**, no. 2, 618–628, doi: [10.1785/0120090085](https://doi.org/10.1785/0120090085).
- Hasselmann, K. (1963). A statistical analysis of the generation of microseisms, *Rev. Geophys.* **1**, no. 2, 177–210.
- Holcomb, G. L. (1989). A Direct Method for Calculating Instrument Noise Levels in Side-by-Side Seismometer Evaluations, *U.S. Geol. Surv. Open-File Rept.* 89-214, 35 pp.
- Longuet-Higgins, M. S. (1950). A theory of the origin of microseisms, *Phil. Trans. Roy. Soc. Lond. A* **243**, no. 857, 1–35, doi: [10.1098/rsta.1950.0012](https://doi.org/10.1098/rsta.1950.0012).
- Marzorati, S., and D. Bindi (2006). Ambient noise levels in north central Italy, *Geochem. Geophys. Geosyst.* **7**, doi: [10.1029/2006GC001256](https://doi.org/10.1029/2006GC001256).
- McNamara, D. E., and R. I. Boaz (2011). PQLX: A Seismic Data Quality Control System Description, Applications, and Users Manual, *U.S. Geol. Surv. Open-File Rept.* 2010-1292, 52 pp.
- McNamara, D. E., and R. P. Buland (2004). Ambient noise levels in the continental United States, *Bull. Seismol. Soc. Am.* **94**, no. 4, 1517–1527, doi: [10.1785/012003001](https://doi.org/10.1785/012003001).
- Meier, U., N. M. Shapiro, and F. Brenguier (2010). Detecting seasonal variations in seismic velocities within Los Angeles basin from correlations of ambient seismic noise, *Geophys. J. Int.* **181**, 985–996, doi: [10.1111/j.1365-246X.2010.04550.x](https://doi.org/10.1111/j.1365-246X.2010.04550.x).
- Peterson, J. (1993). Observation and modeling of seismic background noise, *U.S. Geol. Surv. Open-File Rept.* 93-322, 94 pp.
- Queffeuou, P. (2004). Long-term validation of wave height measurements from altimeters, *Mar. Geodes.* **27**, 495–510, doi: [10.1080/01490410490883478](https://doi.org/10.1080/01490410490883478).
- Rastin, S. J., C. P. Unsworth, K. R. Gledhill, and D. E. McNamara (2012). A detailed noise characterization and sensor evaluation of the North Island of New Zealand using the PQLX data quality control system, *Bull. Seismol. Soc. Am.* **102**, no. 1, 98–113, doi: [10.1785/0120110064](https://doi.org/10.1785/0120110064).
- Ringler, A. T., and C. R. Hutt (2010). Self-noise models of seismic instruments, *Seismol. Res. Lett.* **81**, no. 6, 972–983, doi: [10.1785/gssrl.81.6.972](https://doi.org/10.1785/gssrl.81.6.972).
- Sabra, K. G., P. Gerstoft, P. Roux, W. A. Kuperman, and M. C. Fehler (2005). Surface wave tomography from microseisms in Southern California, *Geophys. Res. Lett.* **32**, L14311, doi: [10.1029/2005GL023155](https://doi.org/10.1029/2005GL023155).
- Stehly, L., M. Campillo, and N. M. Shapiro (2006). A study of the seismic noise from its long-range correlation properties, *J. Geophys. Res.* **111**, B10306, doi: [10.1029/2005JB004237](https://doi.org/10.1029/2005JB004237).
- Trnkoczy, A., P. Bormann, W. Hanka, L. G. Holcomb, R. L. Nigbor, M. Shinohara, K. Suyehiro, and H. Shiobara (2012). Site selection, preparation and installation of seismic stations, in *New Manual of Seismological Observatory Practice (NMSOP-2)*, P. Bormann (Editor), chapter 7, IASPEI, GFZ German Research Centre for Geosciences, Potsdam, Germany, 1–139, doi: [10.2312/GFZ.NMSOP-2](https://doi.org/10.2312/GFZ.NMSOP-2).
- Wessel, P., and W. H. F. Smith (1998). New, improved version of the Generic Mapping Tools released, *Eos Trans. AGU* **79**, 579.

Institute of Geodynamics
National Observatory of Athens
Lofos Nimfon
Athens, 11810, Greece
cevan@noa.gr

Manuscript received 16 November 2011